Measurements of target volumes and organs at risk using DW-MRI in patients with central lung cancer accompanied with atelectasis

XINLI ZHANG[1,2], TONG LIU[3], HONG ZHANG[1] and MINGBIN ZHANG[3]

[1]Department of Medical Oncology, The Affiliated Tai'an City Central Hospital of Qingdao University, Tai'an, Shandong 271000; [2]Department of Radiation Oncology, Shandong Cancer Hospital and Institute, Shandong University, Jinan, Shandong 250117; [3]Department of Stomatology, The Affiliated Tai'an City Central Hospital of Qingdao University, Tai'an, Shandong 271000, P.R. China

Received November 14, 2022; Accepted March 29, 2023

DOI: 10.3892/mco.2023.2641

Abstract. Accurate imaging-based tumor delineation is crucial for guiding the radiotherapy treatments of various solid tumors. Currently, several imaging procedures, including diffusion-weighted magnetic resonance imaging (DW-MRI), intensified computed tomography and positron emission tomography are routinely used for targeted tumor delineation. However, the performance of these imaging procedures has not yet been comprehensively evaluated. In order to address this matter, the present study was conducted in an aim to assess the use of DW-MRI in guiding radiotherapy treatments, by comparing its performance to that of other imaging procedures. Specifically, the exposure dosages to organs at risk, including the lungs, heart and spinal mencord, were evaluated using various radiotherapy regimes. The findings of the present study demonstrated that DW-MRI is a non-invasive and cost-effective imaging procedure that can be used to reduce lung exposure doses, minimizing the risk of radiation pneumonitis. The data further demonstrate the immense potential of the DW-MRI procedure in the precision radiotherapy of lung cancers.

Introduction

The morbidity and mortality rates associated with lung cancer have been increasing annually and lung cancer has become one of the most severe threats to human life and health (1). Due to the lack of early diagnostic tools and the absence of disease symptoms in the early stages of the disease, the majority of patients are diagnosed at an advanced stage (2,3). Central lung cancer refers to tumors that originate in the central part of the lung, including the main bronchus and adjacent structures, and is particularly challenging to treat. Radiotherapy is a standard of care and a curative treatment option for patients with lung cancer. To improve treatment outcomes, dose escalation is routinely used; however, it is frequently associated with the incidence of radiation pneumonitis, a dose-volume-dependent side-effect that is associated with the mean lung dose and the volume of the lung receiving a dose of at least 20 Gy (V_{20}) (4,5). In order to address these challenges, it is crucial to carefully evaluate the risks and benefits of radiotherapy for central lung cancer. By optimizing treatment planning and using appropriate dose constraints, clinicians are able to minimize the risk of radiation pneumonitis and improve disease outcomes for patients with lung cancer.

Precision radiotherapy has become a routine standard of care with the purpose of improving patient outcomes, while mitigating the risk of overdose to target and adjacent organs. The accurate delineation of the gross target volume (GTV) is a crucial step in guiding precision radiotherapy. Several non-invasive imaging procedures have been routinely used for delineating the target volumes of lung cancer (6,7), including intensified computed tomography (CT), positron emission tomography (PET) and diffusion-weighted magnetic resonance imaging (DW-MRI) (8).

However, the CT and PET procedures have inherent limitations. The lack of contrast between soft tissues on CT images can obscure the precision of the radiotherapy by making the distinction of the target area from the normal tissue challenging (9,10), particularly for central lung cancer with pulmonary atelectasis or mediastinal nodes metastasis (11). Although PET has been demonstrated to be more suitable than CT in diagnosing the nodal involvement of lung cancer (7,12,13), it has been reported to produce an increased rate of false-positive results (14). The combination of PET/CT can improve sensitivity and accuracy (7,15,16); however, the previously mentioned challenges remain, including low image resolution and the requirement of PET and CT image fusion (17,18).

Correspondence to: Dr Mingbin Zhang, Department of Stomatology, The Affiliated Tai'an City Central Hospital of Qingdao University, 29 Longtan Road, Tai'an, Shandong 271000, P.R. China
E-mail: zhangmingbin1995@163.com

Key words: diffusion-weighted magnetic resonance imaging, central lung cancer, atelectasis, radiotherapy, organs at risk

DW-MRI is another widely used imaging procedure that provides information concerning the Brownian movement of the water molecules in tissues (19-21). This method can reflect the cellular composition of the tumor and the integrity of the tumor cell membrane (22,23). The differential diffusion of water molecules in tumor tissues enables DW-MRI to detect malignant tumors and differentiate them from benign tissues (24). Previous studies have reported that DW-MRI can provide more accurate delineation for various types of cancer, including prostate cancer, head and neck squamous cell carcinoma, as well as cranial tumors (25-28). The ability of DW-MRI to provide precise and non-invasive imaging render it an attractive option for delineating target volumes in patients with lung cancer. Of note, a previous study by the authors demonstrated that DW-MRI has the potential to reduce exposure doses to organs at risk (OARs), particularly the lungs, and minimizes the risk of radiation pneumonitis (29). These findings suggested that DW-MRI may play a critical role in guiding precision radiotherapy for patients with lung cancer; further research is required to fully investigate its potential for improving patient outcomes.

In three-dimensional conformal radiation treatment (3D-CRT), the accurate delineation of tumor boundaries is challenging, particularly for central lung cancer with atelectasis, when relying solely on intensified CT for target volume delineation. This uncertainty may result in an increased exposure of the surrounding OARs and incidence rates of complications. A previous study by the authors demonstrated that DW-MRI surpassed CT and PET/CT procedures in precise and reproducible delineation of GTVs for lung tumors (29). In the present study, a direct comparison of these three imaging methods is performed in terms of GTV image delineation and the resulting dosages by the lungs, heart, and spinal cord for patients with lung cancer with atelectasis.

Materials and methods

Patient selection. The present study (ethics approval reference no. 2015-06-85) was conducted according to a protocol approved by the Institutional Review Board and the Ethics Committee of Shandong Cancer Hospital and Institute. Written informed consent was obtained from all patients prior to their enrollment in the present study. The critical criterion of patient enrollment is the histological diagnosis of lung cancer accompanied by a varying degree of pulmonary atelectasis. All patients were evaluated for their health condition with a Karnofsky Performance Scale (KPS) score of ≥70 and were deemed eligible for MRI examination with no contraindications. To ensure consistency, all of the images for each patient were collected using the three aforementioned procedures (CT, PET/CT and MRI) within 1 week.

Patient cohort. The present study recruited 27 patients with central lung cancer who were scheduled to undergo precision radiotherapy between October, 2014 and June, 2015, including 23 male and 4 female patients, with the patient age ranging from 37 to 79 years, with a median of 61 years. The lung cancer types included 12 cases of squamous cell carcinoma, six cases of adenocarcinoma, six cases of small cell carcinoma, two cases of atypical carcinoid, and one case of adenoid cystic carcinoma (rare form of adenocarcinoma). Among the 27 patients with central lung cancer, 8 patients presented with tumors in the upper left lung, 4 patients with tumors in the lower left lung, 5 patients with tumors in the upper right lung, 4 patients with tumors in the middle right lung, and 6 patients with tumors in the lower right lung (Table I).

Image acquisition. The images collected using the CT, PET/CT and DW-MRI procedures were acquired and fused according to the methods described in a previous study (29).

GTV delineation on CT, PET/CT and DW-MRI images. GTV measurements obtained according to CT, PET/CT and DW-MRI images, were named as GTV_{CT}, GTV_{PET} and GTV_{MRI}, respectively. All CT, PET/CT, and DW-MRI images were independently reviewed by 10 radiotherapists, and the contours of the tumors were delineated according to standard procedures in China (30). To account for the rough edges of the nodules and clumps in the CT images of lung tumors, the tumor edges were used as a reference for GTV_{CT} delineation. The GTV delineation follows the procedure described in a previous study (29).

Radiotherapy planning. Planning target volume (PTV) was created by expanding the GTV by 5 mm. For each imaging method, simple 3D-CRT plans were developed, namely $Plan_{CT}$, $Plan_{PET}$ and $Plan_{MRI}$. When planning the radiotherapy, the respective center points, the number of shoots, the direction of the field, the frame angle, and the position of the multi-blade grating were set. The dose curve encompassing ≤95% of the PTV was set to receive 95% of the prescribed dose.

All plans were designed for delivery using six MV X-rays, with conventional radiotherapy-30 fractions of 2 Gy to a total dose of 60 Gy administered over a period of 6 weeks. The planning constraints for OARs were set according to the maximum dose administered to the spinal cord was <45 Gy, the mean dose to the lungs was <20 Gy, the percentage of the V_{20} was <30%, the percentage of the total lung volume receiving ≥30 Gy was <20% (V_{30}), and the mean dose to the heart was <20 Gy. The parameters of the lungs, heart and spinal cord were measured and recorded in three sets of radiotherapy plans.

Statistical analyses. Statistical analysis was performed using SAS 9.3 software. The differences between the GTVs and the effects on OARs are summarized as the mean ± mean standard error (SE). The group means of CT, PET/CT and MRI were compared using one-way ANOVA with the Bonferroni adjustment. $P<0.05$ was considered to indicate a statistically significant difference.

Results

Pairwise comparisons of GTV delineation using the CT, PET/CT and DW-MRI methods. The delineated GTVs for the CT, PET/CT and DW-MRI images were obtained through image fusions. DW-MRI images were advantageous in distinguishing central lung cancers from atelectasis, as compared with the T1 and T2 weighted sequence (Fig. 1). In a previous study by the authors (29), examples of images from two individual patients were

Table I. Baseline characteristics of all patients.

Patient no.	Sex	Age, years	Cancer type	Tumor location in lung	Clinical stage
1	Male	62	Squamous cell carcinoma	Upper right	IIIB
2	Male	49	Adenoid carcinoma	Lower right	IIIC
3	Male	62	Squamous cell carcinoma	Upper left	IIIB
4	Male	69	Squamous cell carcinoma	Upper right	IIIB
5	Male	68	Small cell carcinoma	Upper left	IIIB
6	Male	37	Squamous cell carcinoma	Lower right	IIIC
7	Female	41	Small cell carcinoma	Upper left	IIIA
8	Male	65	Atypical carcinoid	Upper left	IIIC
9	Male	69	Squamous cell carcinoma	Lower left	IIIB
10	Male	52	Adenoid carcinoma	Middle right	IIIA
11	Male	52	Small cell carcinoma	Upper right	IIIC
12	Male	65	Small cell carcinoma	Upper left	IIB
13	Male	62	Squamous cell carcinoma	Middle right	IIIB
14	Female	56	Adenoid carcinoma	Lower right	IIIA
15	Male	49	Small cell carcinoma	Lower right	IIIC
16	Male	79	Squamous cell carcinoma	Lower right	IIB
17	Male	74	Squamous cell carcinoma	Lower left	IIIA
18	Male	48	Adenoid carcinoma	Upper left	IIIB
19	Male	61	Small cell carcinoma	Upper left	IIIB
20	Male	48	Squamous cell carcinoma	Lower right	IIIC
21	Male	49	Squamous cell carcinoma	Upper right	IIIC
22	Female	50	Adenoid cystic carcinoma	Lower left	IIIA
23	Female	67	Adenoid carcinoma	Middle right	IIIB
24	Male	65	Atypical carcinoid	Middle right	IIIC
25	Male	53	Adenoid carcinoma	Upper left	IIIB
26	Male	49	Squamous cell carcinoma	Upper right	IIIC
27	Male	67	Squamous cell carcinoma	Lower left	IIIA

Table II. Pairwise comparisons of CT, PET/CT and DW-MRI in lung measurements.

				P-values[a]		
Parameters (mean ± SE)	$Plan_{CT}$	$Plan_{PET}$	$Plan_{MRI}$	CT vs. PET/CT	CT vs. MRI	PET/CT vs. MRI
V_5 (%)	19.28±2.14	15.29±1.98	15.28±2.29	0.011	0.004	NS
V_{10} (%)	14.76±1.76	11.50±1.62	11.57±1.89	0.006	0.002	NS
V_{15} (%)	12.68±1.56	9.52±1.37	9.72±1.59	0.003	0.001	NS
V_{20} (%)	11.19±1.44	8.23±1.21	8.49±1.40	0.002	0.001	NS
V_{25} (%)	9.87±1.39	7.02±1.10	7.32±1.27	0.001	<0.001	NS
V_{30} (%)	8.26±1.31	5.54±0.93	5.94±1.06	0.003	0.003	NS
V_{35} (%)	6.85±1.13	4.12±0.68	4.57±0.82	<0.001	0.001	NS
V_{40} (%)	5.11±0.81	2.74±0.45	3.20±0.57	<0.001	0.001	NS
D_{mean} (cGy)	6.20±0.73	4.50±0.56	4.70±0.68	0.001	<0.001	NS

[a]The P-values were obtained from a one-way ANOVA with Bonferroni adjustment. $Plan_{CT}$, 3D conformal plans in CT imaging; $Plan_{PET}$, 3D conformal plans in PET/CT imaging; $Plan_{MRI}$, 3D conformal plans in MRI imaging; CT, computed tomography; PET, positron emission tomography; MRI, magnetic resonance imaging; V_x, the proportion of lung volume received at least x Gy; D_{mean}, the mean dosage; NS, not significant (P>0.05).

presented. Notably, the GTV delineated from the DW-MRI images was typically smaller in size with clear edges in comparison to the GTVs obtained from the CT and PET/CT images.

Table III. Pairwise comparisons of CT, PET/CT, and MRI in heart measurements.

Parameters (mean ± SE)	$Plan_{CT}$	$Plan_{PET}$	$Plan_{MRI}$	P-values[a]		
				CT vs. PET/CT	CT vs. MRI	PET/CT vs. MRI
V_{30} (%)	8.90±3.61	6.78±3.71	6.59±3.82	NS	0.040	NS
V_{40} (%)	2.86±1.09	1.65±0.88	1.87±1.13	NS	0.036	NS
V_{45} (%)	1.64±0.67	0.85±0.47	1.09±0.68	0.017	0.038	NS
V_{50} (%)	1.14±0.52	0.62±0.36	0.83±0.54	NS	NS	NS
V_{55} (%)	0.87±0.40	0.47±0.28	0.65±0.44	NS	NS	NS
D_{mean} (cGy)	8.16±2.29	5.39±1.88	5.32±1.93	0.007	0.007	NS
D_{max} (cGy)	46.60±6.80	38.42±7.57	38.11±7.72	NS	NS	NS

[a]The P-values were obtained from a one-way ANOVA of least square means with Bonferroni adjustment. $Plan_{CT}$, 3D conformal plans in CT imaging; $Plan_{PET}$, 3D conformal plans in PET/CT imaging; $Plan_{MRI}$, 3D conformal plans in MRI imaging; CT, computed tomography; PET, positron emission tomography; MRI, magnetic resonance imaging; V_x, the proportion of heart volume received at least x Gy; D_{mean}, the mean dosage; D_{max}, the maximum dose; NS, not significant (P>0.05).

Table IV. Pairwise comparisons of CT, PET/CT, and MRI in spinal cord measurements.

Parameters (mean ± SE)	$Plan_{CT}$	$Plan_{PET}$	$Plan_{MRI}$	P-values[a]		
				CT vs. PET/CT	CT vs. MRI	PET/CT vs. MRI
V_{40} (%)	1.13±1.13	0.90±0.90	0.56±0.56	NS	NS	NS
D_{mean} (cGy)	4.91±0.92	4.40±0.86	4.60±0.88	NS	NS	NS
D_{max} (cGy)	27.00±3.78	27.53±3.90	27.93±3.76	NS	NS	NS

[a]The P-values were obtained from a one-way ANOVA with Bonferroni adjustment. $Plan_{CT}$, 3D conformal plans in CT imaging; $Plan_{PET}$, 3D conformal plans in PET/CT imaging; $Plan_{MRI}$, 3D conformal plans in MRI imaging; CT, computed tomography; PET, positron emission tomography; MRI, magnetic resonance imaging; V_{40}, the proportion of spine cord volume received at least 40 Gy; D_{mean}, the mean dose on spine cord; D_{max}, the maximum dose on spine cord; NS, not significant (P>0.05).

Effects on OARs. The radiation doses to the lungs, heart, and spinal cord of cancer patients under various imaging conditions according to $Plan_{CT}$, $Plan_{PET}$, and $Plan_{MRI}$ were obtained, as described in a previous study (29). As demonstrated in Table II, the proportion of lungs in $Plan_{MRI}$ was similar to that in $Plan_{PET}$ for each individual radiation dose, which was significantly reduced as compared with $Plan_{CT}$. Similar results were observed in the dose volume histogram (DVH) of the patients (Fig. 2).

Notably, the data for the heart from all three plans exhibited a similar pattern as that of the lungs, with no statistically significant differences between the three plans (Table III). The proportion of spinal cord volume received in all three plans was similar at the dose of >40 Gy or higher, and the mean and maximum doses on the spinal cord are similar in all three plans (Table IV).

In summary, pairwise comparisons of observed values of the lung for all three plans demonstrated that the DW-MRI values were indistinguishable from those of PET/CT and were differed significantly from those of CT. These data suggested that DW-MRI is appropriate for the delineation of GTVs for central lung cancers with atelectasis.

Discussion

Central lung cancer often simultaneously occurs with obstructive pulmonary atelectasis (31), which makes it imperative to distinguish between the central lung cancer and the accompanying atelectasis when assessing the tumor and delineating the target volume for radiotherapy (19). The incorrect delineation of gross tumor volume could lead to lower survival rates and increased radiation dose on surrounding organs, especially normal lung tissue (32,33).

Whereas CT remains the only 3D imaging modality used for dose calculation, there are limitations in accurately differentiating clinical target volume and gross tumor volume due to low contrast and lack of functional imaging information (34). It is challenging to distinguish lung cancer from pulmonary atelectasis due to inflammation and effusion (35,36). The delineated GTV based on the CT scan images was significantly larger than the pathologic GTV (37). As regards CT, the received dosage of normal lung tissue and other adjacent organs is significantly higher than in PET/CT and MRI (38-39).

PET/CT has been proven to significantly enhance the accuracy of conventional imaging in estimating the full spectrum

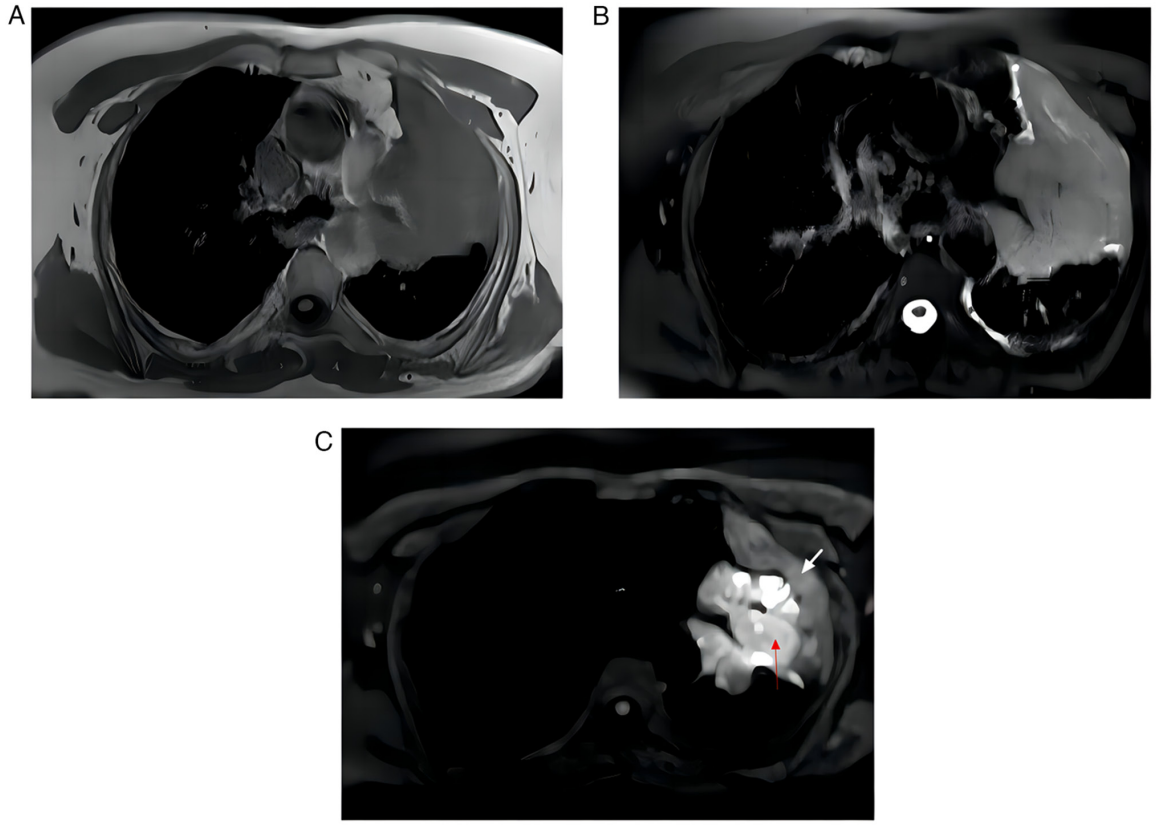

Figure 1. Magnetic resonance imaging sequences of a 61-year-old female patient with a central lung cancer accompanied with atelectasis. (A) Images from T1 sequence. (B) Images from T2 sequence. (C) Images from DWI sequence. DWI can differentiate tumor (red arrow) from atelectasis (white arrow), and tumor in DWI sequence had a clearer margin than those in T1 and T2 sequences. DWI, diffusion weighted imaging.

of lung cancer, as it can distinguish central lung cancer from atelectasis. However, PET/CT can also result in higher radiation exposure and cost (36,38). Deniaud-Alexandre *et al* (40) revealed that PET/CT can provide different GTVs from the traditional CT plan in patients with non-small cell lung cancer and can also change the estimated receiving dosage of heart and lungs.

DW-MRI has become an indispensable tool in cancer research, diagnosis and treatment, and it has been suggested that DWI combined with MRI can provide important information in differentiating lung cancer and atelectasis (41).

In the present study, the mean GTV measurements based on DW-MRI were similar to those based on PET/CT, but smaller than GTV based on CT significantly (29). The results of the present study are consistent with those from previous studies (42-46). DW-MRI outperforms CT in differentiating the central lung cancer from obstructive pulmonary atelectasis and achieves similar outcomes with PET/CT, while avoiding the PET/CT scan radiation and lowering the treatment costs.

In advanced lung cancer precision radiotherapy, the radiation dose is often limited by the amount of exposure to the OARs at the target area. By minimizing the receiving dosage of the OARs, precision radiotherapy can decrease the occurrence of complications and effectively improve the radiation dose of the target area under the same toxicity reaction (30).

Bradley *et al* (47) reported that GTV was positively associated with the average esophageal dose and lung V_{20} in PET/CT delineation of the target area. The results of the present study confirmed that, with the same dose gradient, the exposure volume of the OARs significantly decreased using the DW-MRI-based radiotherapy plan, particularly in lungs. In relation to central lung cancer with atelectasis, with the decrease and disappearance in air content in the lungs, collapsed lung tissues and tumors merge in CT images into a solid mass with a similar density, impeding target delineation in radiotherapy and affecting the receiving dosage of the OARs (29,48). Combined with DW-MRI, the lung atelectasis can be differentiated from the solid lung tumor. The accuracy-boosted delineation of the tumor tissues and the reduced exposure volume of the OARs culminates in lower radiation pneumonitis occurrence rate, a more accomplishable radiotherapy plan, and improved quality of life for patients with lung cancer with atelectasis. Compared to PET/CT, DW-MRI achieved the same effect on the protection of normal lung tissue. The DVH parameters in heart or spinal cord with DW-MRI and PET/CT exhibited a reduced exposure rate in comparison with CT, even though the differences were statistically insignificant.

The limitation of the present study was its small sample size, and further research and larger studies are required for the confirmation of the findings and the evaluation of the benefits of DW-MRI. In conclusion, radiotherapy treatment planning based on DW-MRI plays a crucial role in determining the border of lung cancer with pulmonary atelectasis, precisely delineating GTV, reducing potentially toxic reactions, and improving the quality of life of the patients. Apart

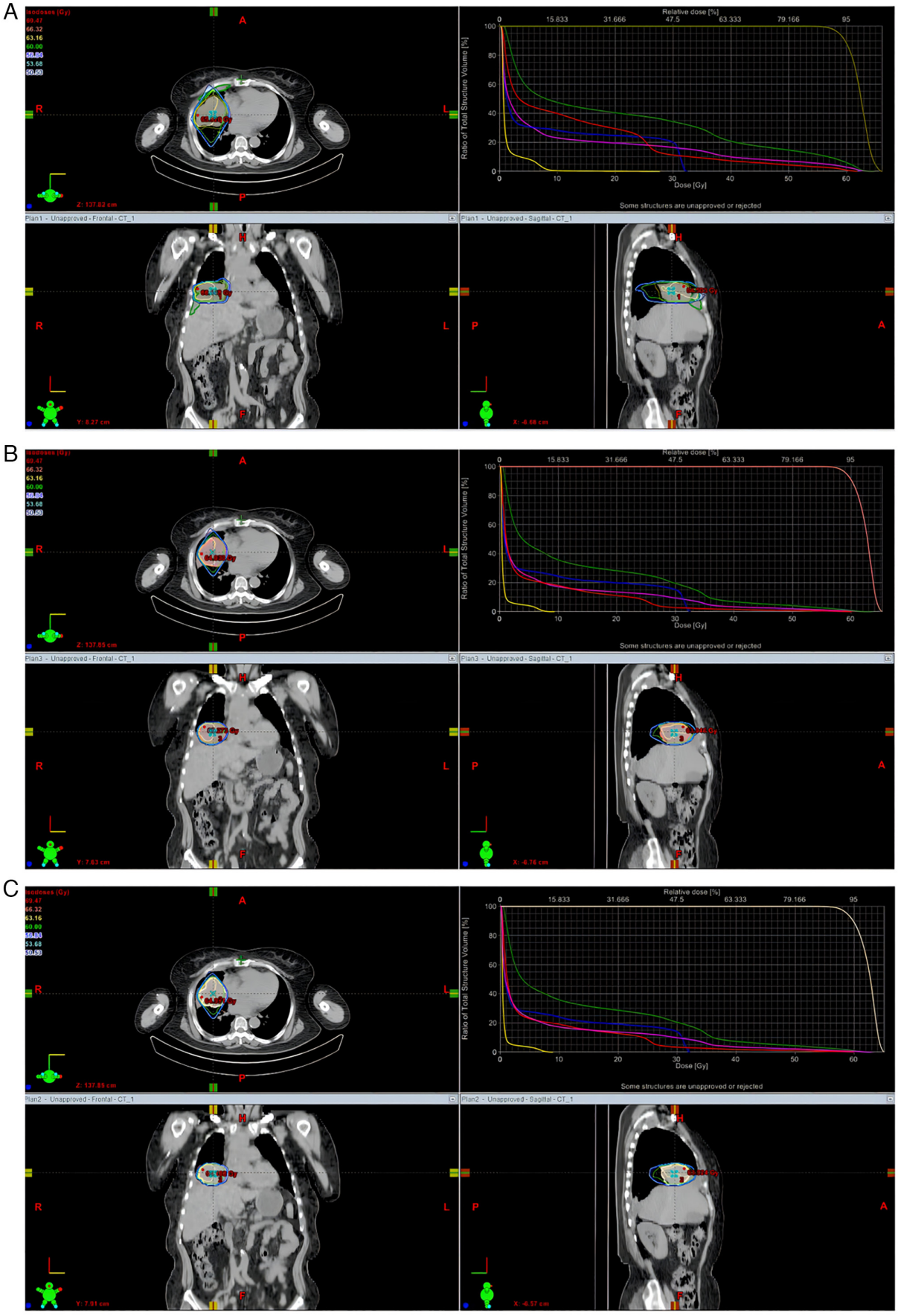

Figure 2. DVH from the (A) $Plan_{CT}$, (B) $Plan_{PET}$ and (C) $Plan_{MRI}$ of a 67-year-old female patient with central lung cancer in right-middle lung. Differences in volume are depicted at every dose under the three plans. The yellow line denotes the left lung, while the right lung, total lung, heart, and spinal cord are respectively represented by the green line (for the right lung), pink line (for the total lung), red line (for the heart) and blue line (for the spinal cord). DVH, dose volume histograms; $Plan_{CT}$, 3D conformal plans in CT imaging; $Plan_{PET}$, 3D conformal plans in PET/CT imaging; $Plan_{MRI}$, 3D conformal plans in MRI imaging; CT, computed tomography; PET, positron emission tomography; MRI, magnetic resonance imaging.

from atelectasis, a number of factors have been reported to affect radiotherapy planning. Patients may achieve more accurate tumor delineation using DW-MRI without sacrificing high-dose radiation on the lungs and heart and spinal cord. DW-MRI is highly recommended since it is radiation-free and more cost-effective, which is particularly important in developing countries. With further research and the development of imaging technologies, DWI-MRI technology may play a more critical role in lung cancer precision radiotherapy.

Acknowledgements

Not applicable.

Funding

The present study was supported by the National Natural Science Foundation of China (NSFC; grant nos. 81272699, 81301936 and 81472811), the Shandong Science and Technology Development Project (grant no. 2014GGC03038) and the International Cooperation Project of Science and Technology Department (grant no. 2012DFA31560).

Availability of data and materials

The datasets used and/or analyzed during the current study are available from the corresponding author on reasonable request.

Authors' contributions

XZ, TL, HZ and MZ were involved in the methodology, data analysis and conceptualization of the study. TL performed the formal analyses and reviewed the manuscript. XZ and HZ wrote and drafted the original manuscript. XZ and MZ confirm the authenticity of all the raw data. All authors have read and approved the final manuscript.

Ethics approval and consent to participate

All patients provided written informed consent prior to enrollment in the study. The study was approved by the Institutional Review Board and the Ethics Committee of Shandong Cancer Hospital and Institute (reference no. 2015-06-85).

Patient consent for publication

All patients provided written informed consent regarding the publication of their data and images.

Competing interests

The authors declare that they have no competing interests.

References

1. Edwards BK, Noone AM, Mariotto AB, Simard EP, Boscoe FP, Henley SJ, Jemal A, Cho H, Anderson RN, Kohler BA, *et al*: Annual Report to the Nation on the status of cancer, 1975-2010, featuring prevalence of comorbidity and impact on survival among persons with lung, colorectal, breast, or prostate cancer. Cancer 120: 1290-1314, 2014.
2. Molina JR, Yang P, Cassivi SD, Schild SE and Adjei AA: Non-small cell lung cancer: Epidemiology, risk factors, treatment, and survivorship. Mayo Clin Proc 83: 584-594, 2008.
3. Shepherd FA, Crowley J, Van Houtte P, Postmus PE, Carney D, Chansky K, Shaikh Z and Goldstraw P; International Association for the Study of Lung Cancer International Staging Committee and Participating Institutions: The International Association for the Study of Lung Cancer lung cancer staging project: Proposals regarding the clinical staging of small cell lung cancer in the forthcoming (seventh) edition of the tumor, node, metastasis classification for lung cancer. J Thorac Oncol 2: 1067-1077, 2007.
4. Martel MK, Ten Haken RK, Hazuka MB, Kessler ML, Strawderman M, Turrisi AT, Lawrence TS, Fraass BA and Lichter AS: Estimation of tumor control probability model parameters from 3-D dose distributions of non-small cell lung cancer patients. Lung Cancer 24: 31-37, 1999.
5. Kong FM, Ten Haken RK, Schipper MJ, Sullivan MA, Chen M, Lopez C, Kalemkerian GP and Hayman JA: High-dose radiation improved local tumor control and overall survival in patients with inoperable/unresectable non-small-cell lung cancer: Long-term results of a radiation dose escalation study. Int J Radiat Oncol Biol Phys 63: 324-333, 2005.
6. Jeon TY, Lee KS, Yi CA, Chung MP, Kwon OJ, Kim BT and Shim YM: Incremental value of PET/CT Over CT for mediastinal nodal staging of non-small cell lung cancer: Comparison between patients with and without idiopathic pulmonary fibrosis. AJR Am J Roentgenol 195: 370-376, 2010.
7. Dwamena BA, Sonnad SS, Angobaldo JO and Wahl RL: Metastases from non-small cell lung cancer: Mediastinal staging in the 1990s-meta-analytic comparison of PET and CT. Radiology 213: 530-536, 1999.
8. Cobben DC, de Boer HC, Tijssen RH, Rutten EG, van Vulpen M, Peerlings J, Troost EG, Hoffmann AL and van Lier AL: Emerging Role of MRI for radiation treatment planning in lung cancer. Technol Cancer Res Treat 15: NP47-NP60, 2016.
9. van Herk M: Errors and margins in radiotherapy. Semin Radiat Oncol 14: 52-64, 2004.
10. Patni N, Burela N, Pasricha R, Goyal J, Soni TP, Kumar TS and Natarajan T: Assessment of three-dimensional setup errors in image-guided pelvic radiotherapy for uterine and cervical cancer using kilovoltage cone-beam computed tomography and its effect on planning target volume margins. J Cancer Res Ther 13: 131-136, 2017.
11. Devic S: MRI simulation for radiotherapy treatment planning. Med Phys 39: 6701-6711, 2012.
12. Toloza EM, Harpole L and McCrory DC: Noninvasive staging of non-small cell lung cancer: A review of the current evidence. Chest 123 (1 Suppl): 137S-146S, 2003.
13. Gould MK, Kuschner WG, Rydzak CE, Maclean CC, Demas AN, Shigemitsu H, Chan JK and Owens DK: Test performance of positron emission tomography and computed tomography for mediastinal staging in patients with non-small-cell lung cancer: A meta-analysis. Ann Intern Med 139: 879-892, 2003.
14. Roberts PF, Follette DM, von Haag D, Park JA, Valk PE, Pounds TR and Hopkins DM: Factors associated with false-positive staging of lung cancer by positron emission tomography. Ann Thorac Surg 70: 1154-1159; discussion 1159-1160, 2000.
15. Silvestri GA, Gould MK, Margolis ML, Tanoue LT, McCrory D, Toloza E and Detterbeck F; American College of Chest Physicians: Noninvasive staging of non-small cell lung cancer: ACCP evidence-based clinical practice guidelines (2nd edition). Chest 132 (3 Suppl): 178S-201S, 2007.
16. Hanna GG, McAleese J, Carson KJ, Stewart DP, Cosgrove VP, Eakin RL, Zatari A, Lynch T, Jarritt PH, Young VA, *et al*: (18)F-FDG PET-CT simulation for non-small-cell lung cancer: Effect in patients already staged by PET-CT. Int J Radiat Oncol Biol Phys 77: 24-30, 2010.
17. Aristei C, Falcinelli L, Palumbo B and Tarducci R: PET and PET-CT in radiation treatment planning for lung cancer. Expert Rev Anticancer Ther 10: 571-584, 2010.
18. Farr KP, West K, Yeghiaian-Alvandi R, Farlow D, Stensmyr R, Chicco A and Hau E: Functional perfusion image guided radiation treatment planning for locally advanced lung cancer. Phys Imaging Radiat Oncol 11: 76-81, 2019.
19. Bourgouin PM, McLoud TC, Fitzgibbon JF, Mark EJ, Shepard JA, Moore EM, Rummeny E and Brady TJ: Differentiation of bronchogenic carcinoma from postobstructive pneumonitis by magnetic resonance imaging: Histopathologic correlation. J Thorac Imaging 6: 22-27, 1991.

20. Maheshwari S and Mukherji SK: Diffusion-weighted imaging for differentiating recurrent cholesteatoma from granulation tissue after mastoidectomy: Case report. AJNR Am J Neuroradiol 23: 847-849, 2002.
21. Moon JY, Kim SH, Choi SY, Hwang JA, Lee JE and Lee J: Differentiating malignant from benign hyperintense nodules on unenhanced T1-weighted images in patients with chronic liver disease: Using gadoxetic acid-enhanced and diffusion-weighted MR imaging. Jpn J Radiol 36: 489-499, 2018.
22. Koh DM and Collins DJ: Diffusion-weighted MRI in the body: Applications and challenges in oncology. AJR Am J Roentgenol 188: 1622-1635, 2007.
23. Iima M: Perfusion-driven intravoxel incoherent motion (IVIM) MRI in Oncology: Applications, challenges, and future trends. Magn Reson Med Sci 20: 125-138, 2021.
24. Usuda K, Zhao XT, Sagawa M, Matoba M, Kuginuki Y, Taniguchi M, Ueda Y and Sakuma T: Diffusion-weighted imaging is superior to positron emission tomography in the detection and nodal assessment of lung cancers. Ann Thorac Surg 91: 1689-1695, 2011.
25. Stieb S, Elgohari B and Fuller CD: Repetitive MRI of organs at risk in head and neck cancer patients undergoing radiotherapy. Clin Transl Radiat Oncol 18: 131-139, 2019.
26. Winter RM, Leibfarth S, Schmidt H, Zwirner K, Mönnich D, Welz S, Schwenzer NF, la Fougère C, Nikolaou K, Gatidis S, *et al*: Assessment of image quality of a radiotherapy-specific hardware solution for PET/MRI in head and neck cancer patients. Radiother Oncol 128: 485-491, 2018.
27. Wee CW, Jang BS, Kim JH, Jeong CW, Kwak C, Kim HH, Ku JH, Kim SH, Cho JY and Kim SY: Prediction of Pathologic findings with MRI-based clinical staging using the bayesian network modeling in prostate cancer: A radiation oncologist perspective. Cancer Res Treat 54: 234-244, 2022.
28. Navarria P, Reggiori G, Pessina F, Ascolese AM, Tomatis S, Mancosu P, Lobefalo F, Clerici E, Lopci E, Bizzi A, *et al*: Investigation on the role of integrated PET/MRI for target volume definition and radiotherapy planning in patients with high grade glioma. Radiother Oncol 112: 425-429, 2014.
29. Zhang X, Fu Z, Gong G, Wei H, Duan J, Chen Z, Chen X, Wang R and Yin Y: Implementation of diffusion-weighted magnetic resonance imaging in target delineation of central lung cancer accompanied with atelectasis in precision radiotherapy. Oncol Lett 14: 2677-2682, 2017.
30. Li Y, Wang L, Gao L, Jin J, *et al*: Radiation Oncology, Version 5.0: 739, 2018.
31. Qi LP, Zhang XP, Tang L, Li J, Sun YS and Zhu GY: Using diffusion-weighted MR imaging for tumor detection in the collapsed lung: A preliminary study. Eur Radiol 19: 333-341, 2009.
32. Senan S and De Ruysscher D: Critical review of PET-CT for radiotherapy planning in lung cancer. Crit Rev Oncol Hematol 56: 345-351, 2005.
33. Yin LJ, Yu XB, Ren YG, Gu GH, Ding TG and Lu Z: Utilization of PET-CT in target volume delineation for three-dimensional conformal radiotherapy in patients with non-small cell lung cancer and atelectasis. Multidiscip Respir Med 8: 21, 2013.
34. Pereira GC, Traughber M and Muzic RF Jr: The role of imaging in radiation therapy planning: Past, present, and future. Biomed Res Int 2014: 231090, 2014.
35. McAdams HP, Erasums JJ, Patz EF, Goodman PC and Coleman RE: Evaluation of patients with round atelectasis using 2-[18F]-fluoro-2-deoxy-D-glucose PET. J Comput Assist Tomogr 22: 601-604, 1998.
36. Schmidt S, Nestle U, Walter K, Licht N, Ukena D, Schnabel K and Kirsch CM: Optimization of radiotherapy planning for non-small cell lung cancer (NSCLC) using 18FDG-PET. Nuklearmedizin 41: 217-220, 2002 (In German).
37. Chan R, He Y, Haque A and Zwischenberger J: Computed tomographic-pathologic correlation of gross tumor volume and clinical target volume in non-small cell lung cancer: A pilot experience. Arch Pathol Lab Med 125: 1469-1472, 2001.
38. Shao Y, Wang H, Chen H, Gu H, Duan Y, Feng A, Li X and Xu Z: Dosimetric comparison and biological evaluation of PET- and CT-based target delineation for LA-NSCLC using auto-planning. Phys Med 67: 77-84, 2019.
39. Chen H, Huang Y, Wang H, Shao Y, Yue NJ, Gu H, Duan Y, Feng A and Xu Z: Dosimetric comparison and biological evaluation of fixed-jaw intensity-modulated radiation therapy for T-shaped esophageal cancer. Radiat Oncol 16: 158, 2021.
40. Deniaud-Alexandre E, Touboul E, Lerouge D, Grahek D, Foulquier JN, Petegnief Y, Grès B, El Balaa H, Keraudy K, Kerrou K, *et al*: Impact of computed tomography and 18F-deoxyglucose coincidence detection emission tomography image fusion for optimization of conformal radiotherapy in non-small-cell lung cancer. Int J Radiat Oncol Biol Phys 63: 1432-1441, 2005.
41. Zhao D, Hu Q, Qi L, Wang J, Wu H, Zhu G and Yu H: Magnetic resonance (MR) imaging for tumor staging and definition of tumor volumes on radiation treatment planning in non-small cell lung cancer: A prospective radiographic cohort study of single center clinical outcome. Medicine (Baltimore) 96: e5943, 2017.
42. Gao Z, Wilkins D, Eapen L, Morash C, Wassef Y and Gerig L: A study of prostate delineation referenced against a gold standard created from the visible human data. Radiother Oncol 85: 239-246, 2007.
43. McLaughlin PW, Evans C, Feng M and Narayana V: Radiographic and anatomic basis for prostate contouring errors and methods to improve prostate contouring accuracy. Int J Radiat Oncol Biol Phys 76: 369-378, 2010.
44. Yang RM, Li L, Wei XH, Guo YM, Huang YH, Lai LS, Chen AM, Liu GS, Xiong WF, Luo LP and Jiang XQ: Differentiation of central lung cancer from atelectasis: Comparison of diffusion-weighted MRI with PET/CT. PLoS One 8: e60279, 2013.
45. Seppala T, Visapaa H, Collan J, Kapanen M, Beule A, Kouri M, Tenhunen M and Saarilahti K: Converting from CT- to MRI-only-based target definition in radiotherapy of localized prostate cancer: A comparison between two modalities. Strahlenther Onkol 191: 862-868, 2015.
46. Bradley J, Bae K, Choi N, Forster K, Siegel BA, Brunetti J, Purdy J, Faria S, Vu T, Thorstad W and Choy H: A phase II comparative study of gross tumor volume definition with or without PET/CT fusion in dosimetric planning for non-small-cell lung cancer (NSCLC): Primary analysis of Radiation Therapy Oncology Group (RTOG) 0515. Int J Radiat Oncol Biol Phys 82: 435-441 e1, 2012.
47. Bradley J, Thorstad WL, Mutic S, Miller TR, Dehdashti F, Siegel BA, Bosch W and Bertrand RJ: Impact of FDG-PET on radiation therapy volume delineation in non-small-cell lung cancer. Int J Radiat Oncol Biol Phys 59: 78-86, 2004.
48. Braun LH, Welz S, Viehrig M, Heinzelmann F, Zips D and Gani C: Resolution of atelectasis during radiochemotherapy of lung cancer with serious implications for further treatment. A case report. Clin Transl Radiat Oncol 9: 1-4, 2017.